Photochemical heating of the mesosphere and lower thermosphere

By B. G. HUNT, *Commonwealth Meteorology Research Centre, P. O. Box 5089AA, Melbourne, Australia, 3001*

ABSTRACT

A diurnally varying photochemical-diffusive model of a neutral oxygen-hydrogen mesosphere and lower thermosphere has been used to calculate the heating rates resulting from the absorption of solar ultraviolet radiation. The model extended from 60 to 160 km and permitted a coherent study to be made of this region, unlike previous investigations. In the thermosphere, where most of the absorption is by O_2, only about 35 % of the solar energy input appeared as local heating. The remainder of the input was primarily removed as chemical energy in the form of a downward flux of atomic oxygen into the mesosphere. This chemical energy was converted into heating by reactions occurring near the mesopause. In the mesosphere, where absorption by O_3 becomes important, a significant amount of the heating is realized indirectly by chemical reactions. An important consequence of this indirect heating is that it continues at night between about 80 and 100 km, unlike the situation in the thermosphere where there is almost no nocturnal heating in the model. Airglow emissions, primarily by electronically excited O_2 in the thermosphere and especially by vibrationally excited OH in the mesosphere, represent important cooling mechanisms in the model. In particular it is estimated that at 88 km. the OH airglow emission could remove about 30 % of the local energy input averaged over 24 hours.

Introduction

A knowledge of the heat budget is fundamental to understanding how the atmosphere functions. For the region under consideration here, 60–160 km, the heat budget is determined by the solar energy input and its subsequent redistribution by chemical reactions, infra-red radiative transfer, diffusive transport of active chemical constituents, meteorological terms (i.e. large scale motions, tides, gravity waves, turbulence) together with other possible mechanisms. In general workers in this field have restricted their studies to specific features of the overall budget. Likewise the present study has been limited to those diurnal heating terms which can be directly calculated with a diffusive-photochemical model of a hydrogen-oxygen mesosphere and lower thermosphere.

Previously Murgatroyd & Goody (1958), Konashenok & Shved (1968), Leovy (1964), Johnson & Gottlieb (1970), Crutzen (1971) amongst others, have considered photochemical heating of this region, normally as part of more general investigations, but with much more limited models than that used here. The present model is derived from an earlier model, Hunt (1971), which was used to calculate the concentrations of the following gases, $O(^3P)$, $O(^1D)$, O_2, O_3, H, OH, HO_2, H_2, H_2O, H_2O_2, and CH_4. In addition to the above gases the concentrations of $O(^1S)$, $O_2(^1\Delta_g)$ and $O_2(^1\Sigma_g^+)$ were calculated in this study, as the determination of the atmospheric heating resulting from photolysis and chemical reactions requires the inclusion of the electronic excitation for the principal gases. These inclusions made very little difference to the concentrations of the 11 original gases. The midday and midnight profiles of the principal gases are plotted in Fig. 1.

Because of the limitation of the model to a neutral hydrogen-oxygen atmosphere, all heating associated with reactions involving nitrogen compounds, ionized constituents and electrons was excluded. Such heating is probably small compared with that of a hydrogen oxygen atmosphere. Also it was assumed that,
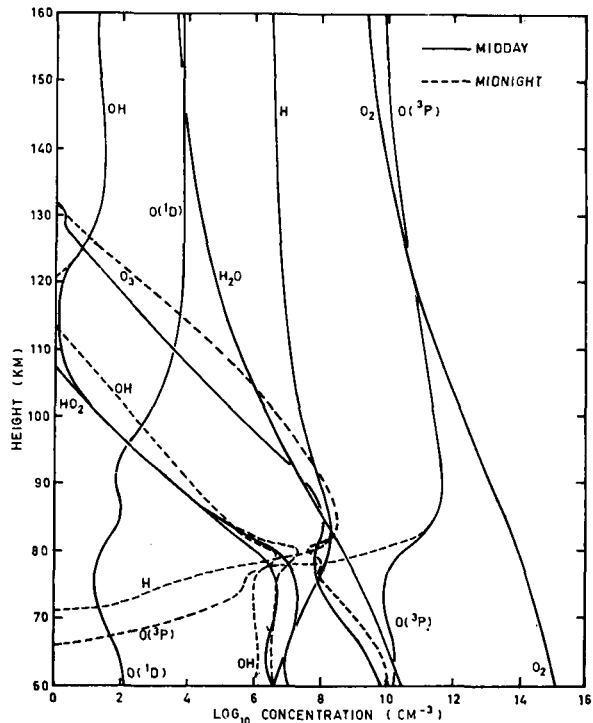
Fig. 1. Midday and midnight concentrations of the principal gases considered in the model.

apart from vibrationally excited OH, any vibrational or rotational excitation was rapidly deactivated to produce local heating of the atmosphere. Some considerations advanced by Crutzen (1971) indicate that this is probably a reasonable assumption for vibrationally excited O_2 above 70 km.

All calculations are for the time of the equinox at the equator.

Reaction scheme

The complete reaction scheme together with the exothermicities of the reactions is given in Tables 1 and 2.

The data for the absorption coefficients and solar radiation intensities are the same as used previously and will therefore not be repeated here. The precise dissociation products of O_2 and O_3 are not known at this time. Thus $O(^1S)$ can result from O_2 dissociation at short enough wavelengths. Also there is some doubt whether $O(^1S)$ and $O_2(^1\Sigma_g^+)$ are produced by dissociation of O_3. The effect of these uncertainties is small as regards the overall heat budget.

In Table 2 the recombination of $O(^3P)$ atoms by reaction 8 has been assumed to follow two paths giving alternative electronically

Table 1. *Photodissociation processes*

No.	Reaction
	$O(^3P) + O(^3P)$, $\lambda < 2, 424$ Å
R 1	$O_2 + h\nu \rightarrow$
	$O(^1D) + O(^3P)$, $\lambda < 1, 750$ Å
	$J_0 = 5.2 \times 10^{-6}$ sec^{-1}
	$O(^3P) + O_2(^3\Sigma_g^-)$, $\lambda < 11, 800$ Å
	$O(^1D) + O_2(^1\Delta_g)$, $\lambda < 3, 100$ Å
R 2	$O_3 + h\nu \rightarrow O(^1D) + O_2(^1\Sigma_g^+)$, $\lambda < 2, 670$ Å
	$O(^1S) + O_2(^1\Delta_g)$, $\lambda < 1, 993$ Å
	$O(^1S) + O_2(^1\Sigma_g^+)$, $\lambda < 1, 800$ Å
	$J_0 = 9.7 \times 10^{-3}$ sec^{-1}
R 3	$H_2O + h\nu \rightarrow H + OH$, $\lambda < 2, 390$ Å
	$J_0 = 1.1 \times 10^{-5}$ sec^{-1}
R 4	$H_2O_2 + h\nu \rightarrow 2OH$, $\lambda < 5, 650$ Å
	$J_0 = 1.5 \times 10^{-4}$ sec^{-1}
	$CH_2 + H_2$, $\lambda < 2, 820$ Å
R 5	$CH_4 + h\nu \rightarrow$
	$CH + H + H_2$, $\lambda < 1, 360$ Å
	$J_0 = 7.3 \times 10^{-6}$ sec^{-1}

For $\lambda < 1$, 360 Å 75 % of the dissociation is assumed to go via the 1st path, 25 % via the 2nd path, see Strobel (1969).

Table 2. *Chemical reactions and their rate constants*

No.	Reaction	Reference
R 6	$O(^3P) + O_2 + M \rightarrow O_3 + M + 25$ kcal $(7.6 \times 10^{-35} \exp (890/RT))$	Benson & Axworthy (1965)
R 7	$O(^3P) + O_3 \rightarrow 2O_2 + 93$ kcal $(5.6 \times 10^{-11} \exp (-5\,700/RT))$	Benson & Axworthy (1965)
R 8a	$O(^3P) + O(^3P) + M \rightarrow O_2 (^1\Sigma_g^+) + M + 80.8$ kcal (10%) (2.7×10^{-33})	See text.
R 8b	$O(^3P) + O(^3P) + M \rightarrow O_2 (^1\Delta_g) + M + 95.8$ kcal (90%)	
R 9	$O_2 + h\nu \rightarrow O_2 (^1\Sigma_g^+) - 37.6$ kcal	Wallace & Hunten (1968)
R 10	$3\ O(^3P) \rightarrow O\ (^1S) + O_2 + 21.8$ kcal (2.0×10^{-34})	Young & Black (1966)
R 11	$O(^1S) \rightarrow O(^1D) + h\nu + 51.2$ kcal (1.4)	Leblanc et al. (1966)
R 12	$O(^1S) + O_2 \rightarrow O(^3P) + O_2 + 96.6$ kcal (2.1×10^{-13})	Zipf (1969)
R 13	$O(^1D) \rightarrow O(^3P) + h\nu + 45.4$ kcal (10^{-2})	Peterson et al. (1966)
R 14	$O(^1D) + O_2 \rightarrow O(^3P) + O_2(^1\Sigma_g^+) + 7.8$ kcal (5.0×10^{-11})	Zipf (1969)
R 15	$O(^1D) + N_2 \rightarrow O(^3P) + N_2 + 45.4$ kcal (7.0×10^{-11})	Zipf (1969)
R 16	$O_2(^1\Sigma_g^+) \rightarrow O_2 + h\nu + 37.6$ kcal (0.085)	Wallace & Hunten (1968)
R 17	$O_2(^1\Sigma_g^+) + N_2 \rightarrow O_2 + N_2 + 37.6$ kcal (1.5×10^{-15})	Zipf (1969)
R 18	$O_2(^1\Sigma_g^+) + O_3 \rightarrow 2O_2 + O(^3P) + 12.4$ kcal (7.1×10^{-12})	Zipf (1969)
R 19	$O_2(^1\Delta_g) \rightarrow O_2 + h\nu + 22.6$ kcal (2.8×10^{-4})	Badger et al. (1965)
R 20	$O_2(^1\Delta_g) + M \rightarrow O_2 + M + 22.6$ kcal (4.3×10^{-19})	Clark & Wayne (1969a)
R 21	$O_2(^1\Delta_g) + O_3 \rightarrow 2O_2 + O(^3P) - 2.6$ kcal $(6.7 \times 10^{-13} \exp (-3100/RT))$	Clark et al. (1970)
R 22	$O_2(^1\Delta_g) + O(^3P) \rightarrow O_2 + O(^3P) + 22.6$ kcal (1.0×10^{-16})	Clark & Wayne (1969b)
R 23	$O(^1S) + H_2O \rightarrow 2OH + 80.0$ kcal (7.0×10^{-11})	Filseth et al. (1970)
R 24	$O(^1D) + H_2O \rightarrow 2OH + 28.8$ kcal (3.0×10^{-11})	Biedenkapp et al. (1970)
R 25	$O(^1D) + H_2 \rightarrow OH + H + 43.6$ kcal (1.9×10^{-10})	Zipf (1969)
R 26	$O(^3P) + H_2 \rightarrow OH + H - 1.8$ kcal $(2.1 \times 10^{-11} \exp (-9400/RT))$	Schofield (1967)
R 27	$O(^1D) + CH_4 \rightarrow CH_3 + OH + 43.7$ kcal (2.2×10^{-10})	Young et al. (1968)
R 28	$O(^3P) + CH_4 \rightarrow CH_3 + OH - 1.7$ kcal $(5.3 \times 10^{-11} \exp (-7950/RT))$	Schofield (1967)
R 29	$H + H + M \rightarrow H_2 + M + 104$ kcal (2.6×10^{-32})	Larkin & Thrush (1964)
R 30	$H + O_2 + M \rightarrow HO_2 + M + 47$ kcal $(2.6 \times 10^{-33} \exp (1600/RT))$	Clyne & Thrush (1963)
R 31	$O(^3P) + OH \rightarrow H + O_2 + 16$ kcal (5.0×10^{-11})	Kaufman (1964)
R 32	$O(^3P) + HO_2 \rightarrow OH + O_2 + 55$ kcal (1.0×10^{-11})	Kaufman (1964)
R 33	$O(^3P) + H_2O_2 \rightarrow OH + HO_2 + 13$ kcal (1.0×10^{-15})	Foner & Hudson (1962)
R 34	$H + O_3 \rightarrow OH + O_2 + 77$ kcal (2.6×10^{-11})	Kaufman (1964)
R 35	$H + HO_2 \rightarrow H_2 + O_2 + 57$ kcal (2.0×10^{-13})	Clyne & Thrush (1963)
R 36	$HO_2 + HO_2 \rightarrow H_2O_2 + O_2 + 42$ kcal (3.0×10^{-12})	Kaufman (1964)
R 37	$OH + HO_2 \rightarrow H_2O + O_2 + 72$ kcal (1.0×10^{-11})	Kaufman (1964)

excited states of O_2, although laboratory substantiation for this assumption is not available. The rate constant for the total path is taken from Reeves et al. (1960), whose measurements were based on the disappearance of $O(^3P)$ atoms. Wallace & Hunten (1968) and Evans et al. (1968) in comparing theoretical and experimental profiles for $O_2(^1\Sigma_g^+)$ and $O_2(^1\Delta_g)$ respectively, concluded that R 8 was the most likely reaction capable of providing a small source required for both of these gases around 90 km. Evans et al. stated that essentially the whole of R 8 was required to go via path (*b*), while Wallace & Hunten needed between 2.5 and 25 % for path (*a*). Arbitrary values of 10 % and 90 % have therefore been assigned here to paths (*a*) and (*b*) respectively. Obviously further laboratory studies are necessary to clarify this situation.

Heating rates at midday and midnight

Illustrated in Fig. 2 are the apparent and actual heating rates at midday owing to the absorption of solar radiation by O_2 and O_3. Photolytic heating by the other gases in the model was negligible. The apparent heating rate is that which would result if all of the absorbed solar radiation was converted immediately into kinetic energy locally in the atmosphere. In actuality a considerable amount of the absorbed radiation goes into chemical energy, which is stored in the dissociation products consequent upon the breaking of the molecular bonds. This can only be transformed into thermal energy by subsequent chemical reaction. Additional energy is also stored as electronic excitation of the dissociation products. When allowance is made for this
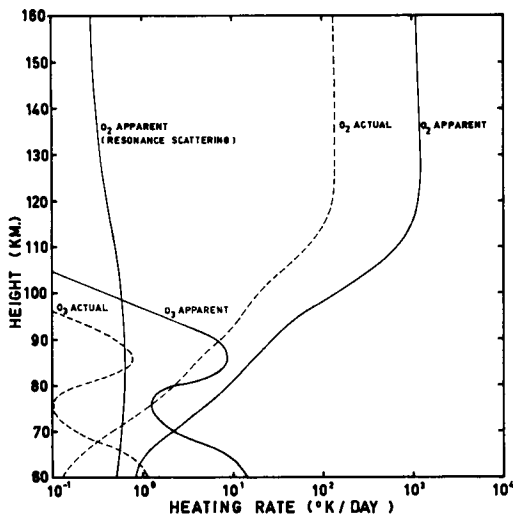
Fig. 2. Apparent and actual heating rates at midday following absorption of solar radiation by O_2 and O_3.

stored energy the actual heating rate is much less than the apparent rate, the respective values at 160 km are approximately 130 and 1 100°K/day for O_2. Similar apparent heating rates have been given by Lagos (1967) for the thermosphere.

Below 110 km the O_2 heating rates decline very rapidly owing to the attenuation of the incident solar radiation capable of dissociating O_2. The variation of the O_3 heating rates in Fig. 2 follows from the O_3 distribution. The kink in the curve around 75 km is associated with a deficit in the O_3 concentration, which resulted from the incorporation of vertical diffusion in the photochemical calculations. This O_3 deficit appears to be a feature of the real atmosphere, although it is undoubtedly over-estimated in the model, Hunt (1971). As for O_2 only about 10 % of the solar radiation absorbed by O_3 produces any immediate heating. The apparent heating produced by resonance excitation of O_2 to $O_2(^1\Sigma_g^+)$ is almost altitude invariant, as indicated in Fig. 2. The actual O_2 heating rate by resonance scattering was not determined, as this requires knowledge of the percentage of the total $O_2(^1\Sigma_g^+)$ formed by resonance scattering, as well as the percentage of the total deactivation which is due to R17 and R18. Although not included in this model absorption of infra red solar radiation by CO_2 can also result in significant heating in the mesosphere according to Houghton (1969).

The heating rates produced by deactivation of the electronically excited states of oxygen are given in Fig. 3; the contribution by $O(^1S)$ was less than 10^{-2} °K/day for the $O(^1S)$ sources included in the model and is omitted from the figure. Since $O(^1D)$ is very efficiently deactivated in the atmosphere by N_2, the solar radiation converted into this electronic excitation by photolysis reappears almost immediately as local heating, being equivalent to a heating rate of approximately 270°K/day at midday in the thermosphere. The sum of the $O(^1D)$ heating rate and the O_2 actual heating rate in Fig. 2 indicates that about 35 % of the initial solar energy absorbed can be considered to constitute local heating in the thermosphere, a similar percentage has been given by Johnson & Gottlieb (1970). The heating resulting from reaction R14 is very much less than that for R15, as the $O(^1D)$ excitation energy is almost entirely converted into electronic excitation of the $O_2(^1\Sigma_g^+)$ molecule formed in the reaction. Heating by the physical deactivation of $O_2(^1\Delta_g)$ and $O_2(^1\Sigma_g^+)$ is small in the thermosphere where their concentrations are low, but in the mesosphere this heating becomes comparable with that of $O(^1D)$ reactions. The variation with height of the heating rates in the mesosphere follows from the O_3 vertical distribution.

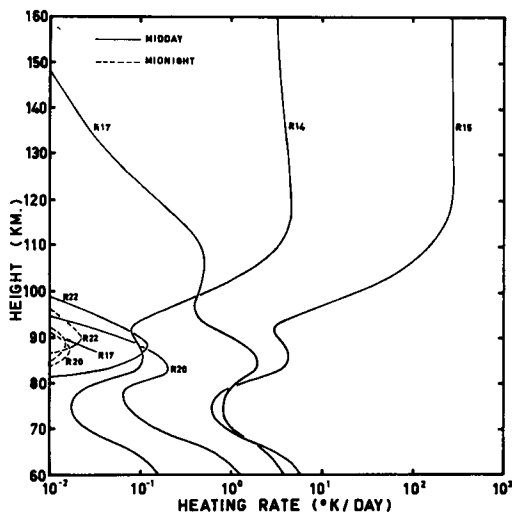The rather insignificant midnight heating rates in Fig. 3 are confined to the upper meso-

Fig. 3. Heating rates at midday and midnight from reactions involving electronically excited forms of oxygen.
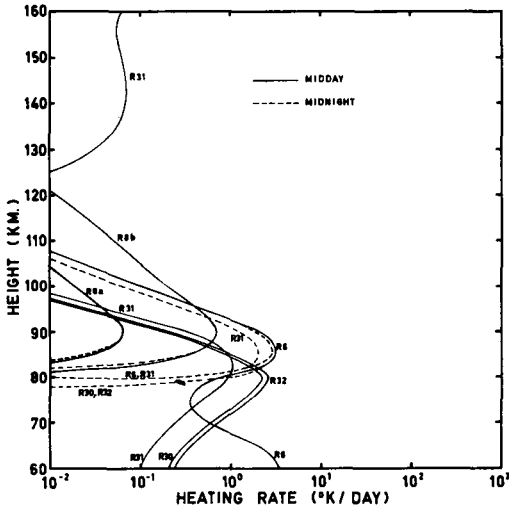
Fig. 4. Heating rates at midday and midnight from neutral hydrogen and oxygen reactions.

sphere, and follow from the low concentrations of $O_2(^1\Delta_g)$ and $O_2(^1\Sigma_g^+)$ calculated by the model after sunset when most of the excitation sources for these gases are terminated.

In Fig. 4 heating by neutral chemical reactions is shown. This heating is important only below about 95 km, the principal contributing reactions at midday being 3-body formation of O_3 and HO_2 and reaction of $O(^3P)$ with HO_2. The nocturnal heating is fairly similar but is relatively more important in view of the smallness of the other heat sources. The dominant reactions are O_3 formation and reaction of $O(^3P)$ with OH and HO_2. Almost no chemical heating occurs below 80 km at night following the reduction of the H and $O(^3P)$ concentrations at these levels, as shown in Fig. 1. The thermospheric heating by reaction R31 follows from the source of OH produced by the reaction of $O(^3P)$ with H_2 in this region, this reaction persists throughout the night. Fairly similar results have been given previously by Konashenok & Shved (1968) for some of these reactions in the mesosphere.

Finally reactions which "cool" the atmosphere have to be considered. The only important reactions in this class are airglow mechanisms, endothermic reactions such as R21 are very minor heat sinks. The airglow emissions cool the atmosphere by radiating the excitation energy of the gases, which would otherwise ultimately

be converted into heat. The airglow cooling rates are illustrated in Fig. 5, the maximum cooling rate of about 20°K/day is attained at 120 km at midday by emission of the oxygen A bands, R16. This rate is very small when compared with the corresponding O_2 apparent heating rate of 1 100°K/day at the same height in Fig. 2. An accurate estimate is impossible in the case of cooling by emission from the vibrationally excited OH formed in the reaction of H and O_3, R34. An upper limit has been given here by assuming that the 77 kcal/mole exothermicity of the reaction is entirely emitted as OH airglow. Since physical deactivation of the excited OH, or reaction with $O(^3P)$, may occur prior to emission the error may be considerable. Crutzen (1971) has considered possible OH deactivation mechanisms in more detail. The maximum apparent cooling by this airglow is at 85 km, with the highest cooling rate of 10°K/day being attained at night. The nocturnal increase in the cooling rate follows from the higher O_3 concentrations at this time, see Fig. 1, while the marked reductions in the H concentrations below 80 km at night severely restricts the OH airglow cooling in this region.

The remaining heating term which can be estimated from the model is that associated with the diffusive fluxes, although only the heating resulting from the transport of chemical energy is considered here. Only the $O(^3P)$ diffusive flux had any significant thermal
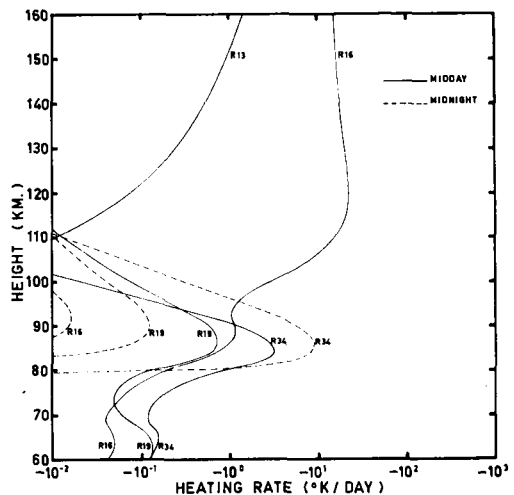

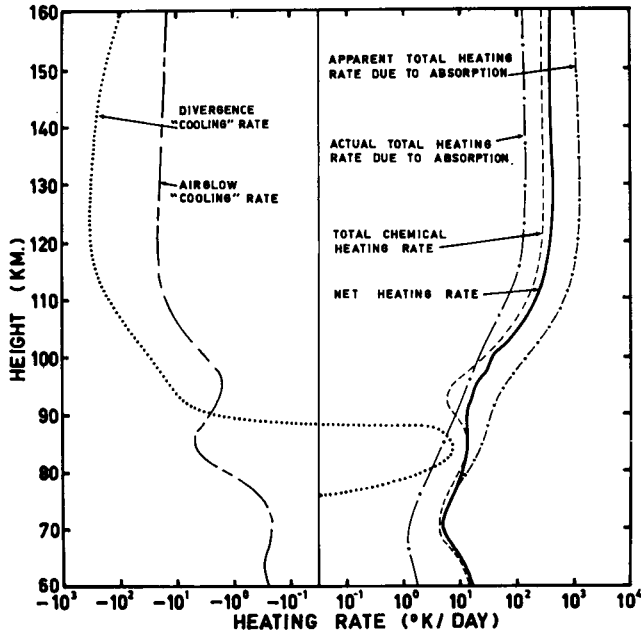*Fig. 5.* "Cooling" rates at midday and midnight associated with airglow emissions.

Fig. 6. The variation with height at midday of the total radiative and reactive heating rates and the "cooling" rates due to airglow emission and divergence of atomic oxygen.

effect in the model, producing a large apparent cooling of about 300°K/day near 130 km, as shown in Fig. 6. The convergence of this flux in the mesosphere was equivalent to a very much smaller heating rate because of the larger atmospheric density there. Although the O(^{3}P) flux is shown as a cooling rate in the thermosphere, the removal of the O(^{3}P) chemical energy by itself does not produce any cooling. However it does prevent this energy from appearing as heating, which would happen if sufficient time was available for reaction.

Also shown in Fig. 6 are the midday total heating rates for each mechanism and the net heating rate. The grand total heating rate, not given in Fig. 6, is the sum of the total chemical and total actual radiative heating rates. The difference between this grand total heating rate and the total airglow cooling rate was used to define the net heating rate in the figure. The importance of the divergence cooling can be assessed from this figure, as in the absence of this mechanism the heating rate would be nearly doubled to approach that of the apparent solar absorption rate over much of the thermosphere. In fact only below about 80 km is the net heating rate equal to the

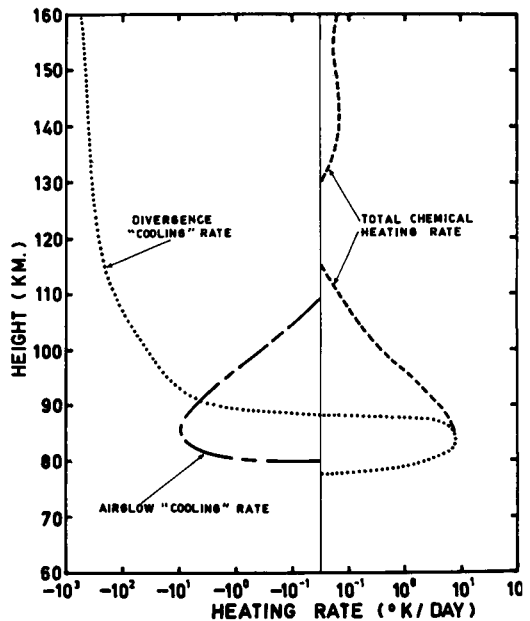apparent solar absorption heating rate. Note that the sum of the heating and cooling rates

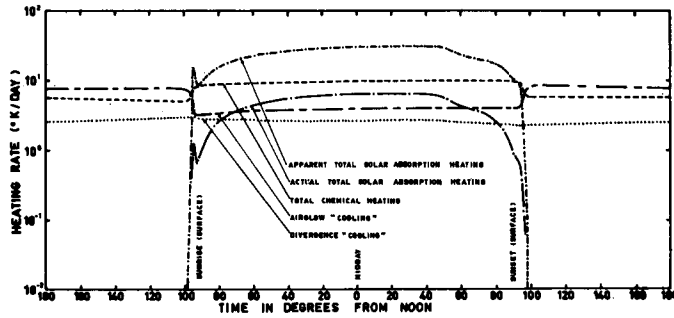*Fig. 7.* As for Fig. 5 but at midnight.

Fig. 8. The diurnal variation of the various heating components at 88 km.

is not equal to the apparent solar absorption heating rate in the thermosphere at midday, as the $O(^3P)$ concentration is increasing at this time and thus storage of chemical energy results.

The corresponding midnight situation is shown in Fig. 7. The $O(^3P)$ divergence curve is almost time invariant and illustrates the importance of this term in the heat balance of the thermosphere. Only neutral chemical reactions are important as heat sources in the model at night, hence the thermospheric heating rate is very much smaller than at midday. In the mesosphere the major change is the drastic reduction of reactions below about 80 km; the airglow cooling rates are very nearly equal to the chemical heating rates in this region.

Diurnal variations

In the thermosphere the diurnal variations of the total radiative and reactive constituents identified in Figs. 6 and 7 are virtually step-functions symmetrical about midday, with ordinates in the sunset and sunrise periods. Consequently the heating rates averaged over a day are very nearly one-half the midday rates given in Fig. 6. Above about 120 km the daily mean net heating rate is approximately 190°K/day, which should be contrasted with the midday apparent radiative heating rate of 1 100°K/day. Part of this net heating rate is counteracted by thermal conduction and other mechanisms, and part appears as a diurnal variation of the thermospheric temperature,

estimates of which are available in the CIRA 1965 model atmosphere. The divergence "cooling" by the $O(^3P)$ flux has a much smaller diurnal variation than the other heating terms. At 160 km there is a 20-fold variation with a minimum in the afternoon and a maximum at dawn.

The situation at 88 km is illustrated in Fig. 8. The two radiative heating curves are not symmetrical about midday owing to variations in the O_3 concentration near sunset and sunrise. At these times the heating by O_2 is very small as the very long pathlengths involved attenuate the relevant wavelengths. "Spikes" appear in the radiative curves at dawn, as noted previously by Leovy (1964), resulting from the destruction of the nocturnal O_3 increase in this region. The divergence term, which is actually a heating term at 88 km, is almost time invariant with most of the heating being realized by reaction R6. The higher chemical reaction heating during the day compared to the night results primarily from deactivation of $O(^1D)$ and $O_2(^1\Sigma_g^+)$; at night these gases virtually disappear. Crude estimates of the daily mean heating rates from Fig. 8 indicate that the total heat input is about 15°K/day, the actual heating rate being 10°K/day and the airglow cooling rate 5°K/day. Thus about one third of the heat input at 88 km may not be realized as local heating. Extensive estimates of the diurnal heating rates in the mesosphere based on apparent solar absorption by O_2 and O_3 have been presented by Murgatroyd & Goody (1958). In addition Leovy (1967) has made a rough estimate of the heat budget of this region based on the known sources and sinks of energy.

Conclusions

This study represents only one of the many facets of determining the heat budget of the mesosphere and lower thermosphere. Estimates of some of the other components of the budget will be more difficult to obtain, but are necessary before this region of the atmosphere can be adequately modelled.

REFERENCES

Badger, R. M., Wright, A. C. & Whitlock, R. F. 1965. Absolute intensities of the discrete and continuous absorption bands of oxygen gas at 1.26 and 1.065 μ and the radiative lifetime of the $^1\Delta_g$ state of oxygen. J. Chem. Phys. 43, 4345.

Benson, S. W. & Axworthy, A. E. 1965. Reconsideration of the rate constants from the thermal decomposition of ozone. J. Chem. Phys. 42, 2614–2615.

Biedenkapp, D., Hartshorn, L. G. & Bair, E. J. 1970. The $O(^1D) + H_2O$ reaction. Chem. Phys. Lett. 5, 379–380.

Clark, I. D. & Wayne, R. P. 1969a. Collisional quenching of $O_2(^1\Delta_g)$. Proc. Roy. Soc. A 314 111–127.

Clark, I. D. & Wayne, R. P. 1969b. The reaction of $O_2(^1\Delta_g)$ with atomic nitrogen and with atomic oxygen. Chem. Phys. Lett. 3, 405–407.

Clark, I. D., Jones, I. T. N. & Wayne, R. P. 1970. The kinetics of the reaction between $O_2(^1\Delta_g)$ and ozone. Proc. Roy. Soc. A 317, 407–416.

Clyne, M. A. A. & Thrush, B. A. 1963. Rates of elementary processes in the chain reaction between hydrogen and oxygen 2. Kinetics of the reaction of hydrogen atoms with molecular oxygen. Proc. Roy. Soc. A 275, 559–566.

Crutzen, P. J. 1971. Energy conversions and mean vertical motions in the high latitude summer mesosphere and lower thermosphere in Mesospheric Models and Related Experiments, Reidel, Holland.

Evans, W. F. J., Hunten, D. M., Llewellyn, E. J. & Vallance Jones, A. 1968. Altitude profile of the infrared atmospheric system of oxygen in the dayglow. J. Geophys. Res. 73, 2885–2896.

Filseth, S. V., Stuhl, F. & Welge, K. H. 1970. Collisional deactivation of $O(^1S)$. J. Chem. Phys. 52, 239–243.

Foner, S. N. & Hudson, R. L. 1962. Mass spectrometry of the HO_2 free radical. J. Chem. Phys. 36, 2681–2690.

Houghton, J. T. 1969. Absorption and emission by carbon-dioxide in the mesosphere. Quart. J. Roy. Met. Soc. 95, 1–20.

Hunt, B. G. 1971. A diffusive-photochemical study of the mesosphere and lower thermosphere and the asssociated conservation mechanisms. J. Atmosph. Terr. Phys. 33, 1869–1892.

Johnson, F. S. & Gottlieb, B. 1970. Eddy mixing and circulation at ionospheric levels. Planet. Space Sci. 18, 1707–1718.

Kaufman, F. 1964. Aeronomic reactions involving hydrogen. A review of recent laboratory studies. Ann. Geophys. 20, 106–114.

Konashenok, V. N. & Shved, G. M. 1968. On the physical conditions near the mesopause. Atoms. Ocean Phys. 4, 277–281.

Lagos, C. P. 1967. On the dynamics of the thermosphere. M.I.T. Dept. of Meteorology, Planetary Circulations Project, Report No. 20.

Larkin, F. S. & Thrush, B. A. 1964. Recombination of hydrogen atoms in the presence of atmospheric gases. Disc. Faraday Soc. 37, 113–117.

Leblanc, F. J., Oldenburg, O. & Carleton, N. P. 1966. Transition probabilities of forbidden oxygen lines in a discharge tube. J. Chem. Phys. 45, 2200–2003.

Leovy, C. 1964. Radiative equilibrium of the mesosphere. J. Atmosph. Sci. 21, 238–248.

Leovy, C. 1967. Energetics of the middle atmosphere. Paper presented at Survey Symposium on Measurements in the Upper Atmosphere (ICMUA, IAMAP), XIV General Assembly of IUGG, Switzerland.

Murgatroyd, R. J. & Goody, R. M. 1958. Sources and sinks of radiative energy from 30 to 90 km. Quart. J. Roy. Met Soc. 84, 225–234.

Peterson, V. L., Vanzandt, T. E. & Norton, R. B. 1966. F-region nightglow emissions of atomic oxygen. I. Theory. J. Geophys. Res. 71, 2555–2265.

Reeves, R. R., Manella, G. & Harteck, P. 1960. Rate of recombination of oxygen atoms. J. Chem. Phys. 32, 632–633.

Schofield, K. 1967. An evaluation of kinetic rate data for reactions of neutrals of atmospheric interest. Planet Space Sci. 15, 643–670.

Strobel, D. F. 1969. The photochemistry of methane in the Jovian atmosphere. J. Atmosph. Sci. 26, 906–911.

Wallace, L. & Hunten, D. M. 1968. Dayglow of the oxygen A band. J. Geophys. Res. 73, 4813–4834.

Young, R. A. & Black, G. 1966. Excitation of the auroral green line in the earth's nightglow. Planet Space Sci. 14, 113–116.

Young, R. A., Black, G. & Slanger, T. G. 1968. Reaction and deactivation of $O(^1D)$. J. Chem. Phys. 49, 4758–4768.

Zipf, E. C. 1969. The collisional deactivation of metastable atoms and molecules in the upper atmosphere. Can. J. Chem, 47 .1863–1870.

ФОТОХИМИЧЕСКИЙ НАГРЕВ МЕЗОСФЕРЫ И ХИЖНЕЙ ТЕРМОСФЕРЫ.

Фотохимически-диффузионная модель нейтральной кислородноводородной мезосферы и нижней термосферы с учетом суточного хода была использована для вычисления скоростей нагревания, благодаря поглощению солнечной ультрафиолетовой радиации. Модель простирается от 60 до 160 км и позволяет провести, в отличие от предыдущих исследований, согласованное изучение этой области. В термосфере, где большая часть поглощения обусловлена O_2, только около 35% подводимой солнечной энергии проявляется в локальном нагревании. Остальная часть энергии отводится, главным образом, в виде химической энергии направленного вниз в мезосферу потока атомарного кислорода. Эта химическая энергия превращается в тепло при реакциях, происходящих вблизи мезопаузы. В мезосфере, где поглощение озоном становится существенным, значительная величина нагревания реализуется непрямым образом при химических реакциях. Важным следствием этого непрямого нагрева является то, что он продолжается и ночью на высотах между, приблизительно, 80 и 100 км, в отличие от ситуации в термосфере, где в данной модели почти нет нагревания ночью. Эмиссии свечения воздуха, главным образом, электронно возбужденного O_2 в термосфере и, особенно, вибрационно возбужденного OH в термосфере, представляют в модели важные механизмы охлаждения. В частности, оценено, что на высоте 88 км свечение OH может удалить около 30% локального подвода энергии, осредненного за сутки.